

1 **Observationally constrained analysis of sea salt aerosol in the**  
2 **marine atmosphere**

3  
4 Huisheng Bian<sup>1,2</sup>, Karl Froyd<sup>3,4</sup>, Daniel M. Murphy<sup>3</sup>, Jack Dibb<sup>5</sup>, Mian Chin<sup>2</sup>, Peter R. Colarco<sup>2</sup>,  
5 Anton Darmenov<sup>2</sup>, Arlindo da Silva<sup>2</sup>, Tom L. Kucsera<sup>6</sup>, Gregory Schill<sup>3,4</sup>, Hongbin Yu<sup>2</sup>, Paul  
6 Bui<sup>7</sup>, Maximilian Dollner<sup>8</sup>, Bernadett Weinzierl<sup>8</sup>, and Alexander Smirnov<sup>9</sup>

7 <sup>1</sup> University of Maryland at Baltimore County, Baltimore County, MD

8 <sup>2</sup> NASA Goddard Space Flight Center, Greenbelt, MD

9 <sup>3</sup> NOAA Earth System Research Laboratory, Chemical Sciences Division, CO

10 <sup>4</sup> Cooperative Institute for Research in Environmental Sciences, University of Colorado, Boulder, CO

11 <sup>5</sup> University of New Hampshire, Durham, NH

12 <sup>6</sup> Universities Space Research Association, Columbia, MD

13 <sup>7</sup> NASA Ames Research Center, Moffett Field, CA

14  
15 <sup>8</sup> University of Vienna, Faculty of Physics, Aerosol and Environmental Physics, Boltzmanngasse 5, A-  
16 1090 Wien, Austria

17  
18 <sup>9</sup> Science Systems and Applications, Inc., Lanham, MD 20706  
19

20  
21 **Supplementary Material**

22  
23 **Three sea salt emission algorithms used in GEOS GOCART**

24 A lot of effort has been devoted to develop and improve the parameterization of sea salt  
25 emission algorithms, which are primarily dependent on wind speed, atmospheric stability,  
26 sea surface and air temperatures, and salinity in the near-surface ocean waters (Lewis and  
27 Schwartz, 2004; Barthel et al., 2014). Here we examine three of the sea salt emission

28 schemes that have been implemented in GEOS/GOCART: 1) a scheme proposed by  
29 Gong (2003) (named Emi1), 2) a derivative of Gong's parameterization with a modified  
30 wind source term developed at the NASA Global Modeling and Assimilation Office  
31 (GMAO) using Moderate Resolution Imaging Spectroradiometer (MODIS) AOD over  
32 vast oceans (Emi2), and 3) the sea salt emission scheme used in the Modern-Era  
33 Retrospective Analysis for Research and Applications version 2 (MERRA2) reanalysis  
34 that has the same wind source function as Emi2 but also includes a sea surface  
35 temperature correction tailored to GEOS (Emi3). Emi1 is the sea salt emission that is  
36 widely used by aerosol community (Jaeglé et al. 2011; Spada et al., 2015; Textor et al.,  
37 2006). Emi3, which is derived based on Emi1 and Emi2, is the current default sea salt  
38 emission used by GEOS GOCART in the sea salt simulations presented in the main body  
39 of this paper. A Tom global surveys, by providing comprehensive and independent sea  
40 salt observations, allow us to confirm that the Emi3 is indeed an improved emission.

41

42 Details for Emi2 and Emi3 are described here. Sea salt emissions are controlled by  
43 aerosol particles generated from collapsing bubbles and ejected jet droplets that in turn  
44 are directly related to the whitecap fraction in the ocean and are commonly parameterized  
45 as a function of wind speed and SST. In global models this functional dependence is  
46 further simplified and expressed as the product of 10-m wind ( $W(u_{10m})$ ), SST ( $T(SST)$ ),  
47 and size distribution terms ( $S(D)$ ), e.g., number flux:

48

$$49 \frac{dN}{dD} = W(u_{10m}) T(SST) S(D)$$

50

51 The  $W(u_{10m})$  and  $S(D)$  are described in Gong (2003) as:

52  $W(u_{10m}) = u_{10}^{3.41}$

53  $S(D) = (1 + 0.057r^{1.05}) \times 10^{1.19e^{-B^2}}$

54 Where  $B = (0.380 - \log r)/0.650$ . The Emi2 in GEOS uses the size distribution of Gong  
55 (2003), wind forcing term proportional to  $u_*^{2.41}$  (where  $u_*$  is the friction velocity). The  
56 default sea salt emissions scheme Emi3 in GEOS further accounts for a SST correction  
57 term derived from AOD over the oceans (Randles et al., 2017).

58

59 The  $T(SST)$  in Emi3 is

60  $T(SST) =$

61  $(-1.107211 - 0.010681 * \text{tskin\_c} - 0.002276 * \text{tskin\_c}^2 + 60.288927 * 1.0 / (40.0 -$   
62  $\text{tskin\_c}))$

63 Here  $\text{tskin\_c}$  is the sea surface skin temperature in Celsius.  $\text{tskin\_c}$  is set to be -0.1 when  
64 below -0.1 and to be 36.0 when above 36.0. Furthermore, the overall temperature  
65 modification  $\text{fsstemis}$  is confined within 0.0 to 7. Note that the Emi3 is the default  
66 emission currently used in GEOS.

67

68 Figure S1 shows the point-to-point comparison of sea salt between ATom PALMS  
69 measurements and the GEOS model simulation using the three described emissions along  
70 aircraft flight tracks of ATom1 and ATom2, respectively. Several order shifts of sea salt  
71 magnitude shown by both measurement and simulation reflect the presence of a strong  
72 sea salt vertical gradient within the troposphere. All three emission methods give higher  
73 sea salt mass concentrations where the peak values occurred, implying possible

74 overestimation of emissions. Statistical analysis given in table S1 indicates that sea salt  
75 simulated by GEOS, over all sampling points of PALMS, is about 1.2 to 2 times higher in  
76 ATom1 and 2 to 3 times higher in ATom2 depending on which emission algorithm is  
77 used.

78

79 To have an accurate sea salt emission, the most important thing is to have a good wind  
80 parameterization since wind is the fundamental driver to generate sea spray particles. By  
81 using surface friction velocity (Emi2) instead of the 10-m wind (Emi1), the correlation  
82 coefficient was increased from 0.50 to 0.54 in ATom1 and from 0.38 to 0.43 in ATom2.  
83 This makes sense since surface friction velocity is more physically meaningful than the  
84 10-m wind for sea salt wind-borne emissions.

85

86 The correlation coefficients are further lifted up to 0.60 (ATom1) and 0.50 (ATom2)  
87 when SST-correction is applied (Emi3, the default emission). Several previous studies  
88 have reported that simulated sea salt emission is affected by sea surface temperature.  
89 Spada et al. (2013) run an online CTM model to examine five sea salt emission  
90 algorithms and found that SST-dependent emission schemes lead to a clear improvement  
91 of surface sea salt simulation when compared with measurements of Aerosol  
92 Robotic Network (AERONET), University of Miami's Ocean Aerosol Network, and two  
93 NOAA Pacific Marine Environmental Laboratory (PMEL) cruises. Salter et al., (2015)  
94 proposed a size-resolved particle algorithm and found that total number density decrease  
95 nonlinearly with increasing seawater temperature, but other sea salt properties (e.g.  
96 effective radius, surface area, volume and mass) increase with increasing seawater

97 temperature due to increased production of particles with dry diameters greater than 1  
98  $\mu\text{m}$ . Jaeglé et al. (2011) used cruise observations to derive an empirical temperature  
99 corrected sea salt source function in GEOS-Chem, which resulted in better agreement  
100 between simulation and measurements from in situ cruises, MODIS and AERONET  
101 AOD. A contradictory conclusion, i.e. no apparent relationship between water  
102 temperature and measured sea-salt concentration, however, was found in the analyzed  
103 data set, which contained open-ocean shipboard measurements from five different  
104 campaigns covering the South Indian Ocean, the Western Pacific region, the New  
105 England region, and the Gulf of Maine by the PMEL group (Witek et al., 2007). Overall,  
106 inclusion of SST-correction indeed improves sea salt simulation on a global scale at least  
107 during the summer and winter seasons. Furthermore, the three emission algorithms  
108 discussed in supplementary section show that the uncertainty among the model  
109 simulations is generally less than the difference between model and measurement.

110

111

112

### 113 **Figure Captions**

114 **Figure S1a.** Sea salt mass concentration with particle diameter ( $D_p$ ) less than 3  $\mu\text{m}$  along  
115 ATom1 flight track. Black line is for PALMS measurement, while color lines represent  
116 the GEOS model simulation with three different emission algorithms. Note Emi3 is  
117 currently default emission algorithm used in the GEOS model.

118

119 **Figure S1b.** similar to Fig. 2a but for ATom2.

120

121

122  
123

**Table S1.** Statistical analysis of the sea salt results from the ATom PALMS and SAGA measurements and GEOS5 simulation along flight tracks in ATom1 and ATom2

	Emission algorithm	GEOS – PALMS		
		R	Bias	NRMS
ATom1	Emi1	0.50	1.21	0.11
	Emi2	0.54	2.06	0.15
	Emi3	0.60	2.01	0.15
ATom2	Emi1	0.38	2.00	0.14
	Emi2	0.43	3.09	0.19
	Emi3	0.50	2.55	0.15

124  
125

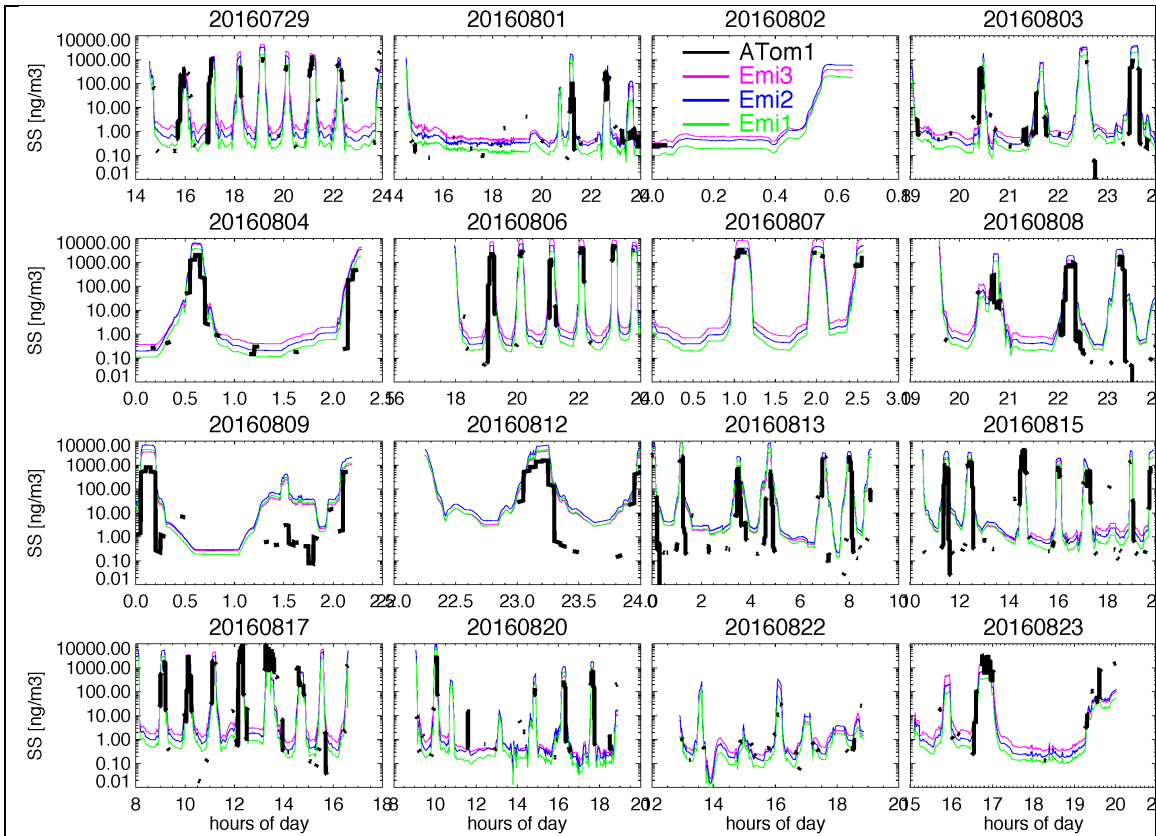


**Figure S1a.** Sea salt mass concentration with particle diameter ( $D_p$ ) less than  $3 \mu\text{m}$  along ATom1 flight track. Black line is for PALMS measurement, while color lines represent the GEOS5 model simulation with three different emission algorithms. Note Emi3 is currently default emission algorithm used in the GEOS5 model.

126  
127

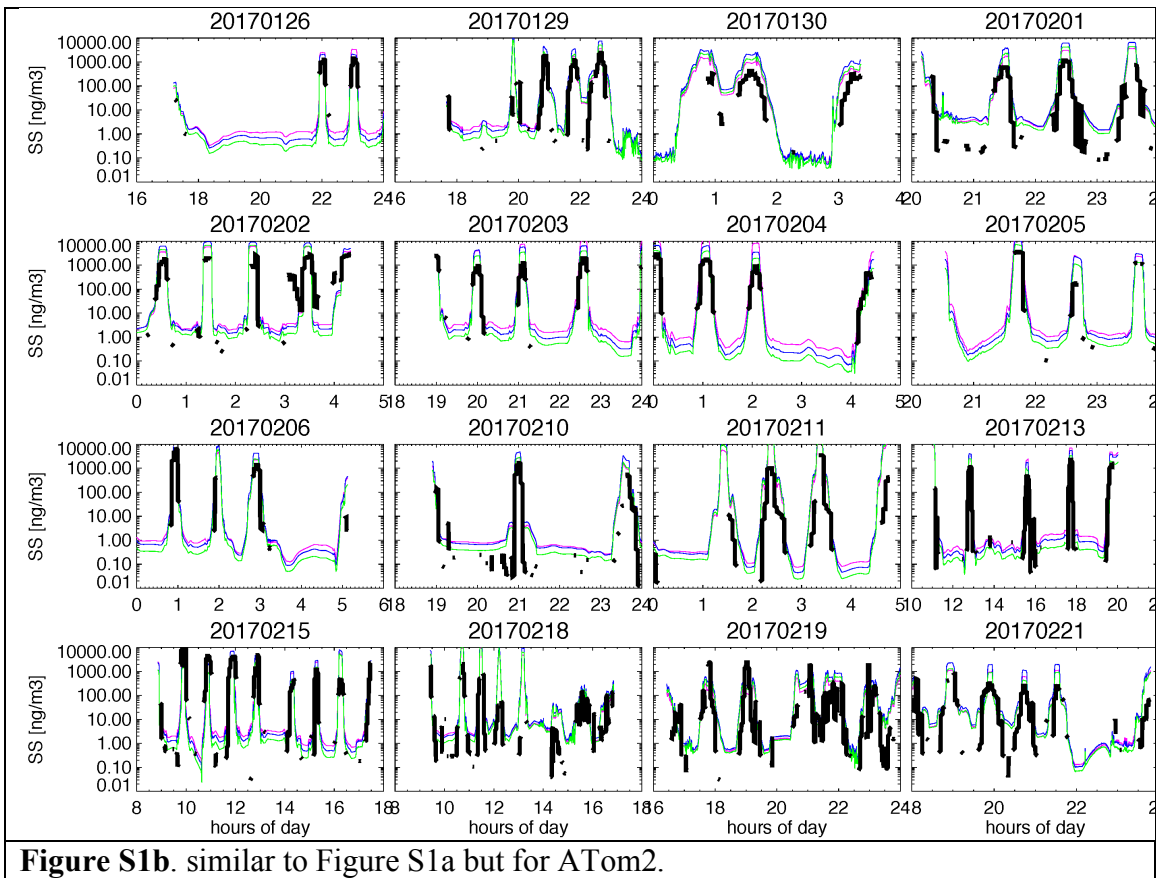


**Figure S1b.** similar to Figure S1a but for ATom2.